So far we've dealt with

- Discretization of *time* using finite difference method (Taylor expand points and combine)
- Discretization of *energy* using the multigroup approximation, where we assume group-integrated values.
- *Expanding sources*, in particular scattering, in spherical harmonics–which we reduce to Legendre Polynomials in the case of azimuthal symmetry.
- Discretization of *angle* using either
    - S_N: get solutions along specific angle sets (quadrature points), use corresponding quadrature weights to integrate over angle
    - P_N: expand the angular flux in spherical harmonics, which we only do in 1-D so Legendre polynomials in practice, and solve a set of coupled equations for each expansion term (with closure relations at $n = 0 and n = N + 1$).
    - SP_N: we take the 1-D P_N equations and transform them to 3D by replacing the 1-D diffusion operators with the 3-D diffusion operator and replacing the derivatives at the boundary with the outward normal derivatives. We also replace $\phi_{l'}$ by a vector for odd l'.

When we do all of this we get $t = 0, \ldots, T$ equations in time, $g = 0, \ldots, G$ equations in energy, and a number of equations in angle that depends on which approach we take. However, we still have one major item to deal with...

Space

(Largely from Evans, some from Vujíc)

There are *many* spatial discretization choices out there. What you choose can depend on the geometry and physical properties, as well as if you're using Cartesian or curvilinear formulations. Fundamentally, we can characterize the differencing schemes in a few ways

- cell balance, which includes
    - Finite Difference Method (FDM) – using point value solution

- **–** Finite Volume Method (FVM) – using cell-averaged value solution
- finite element (FEM) – using basis function for expansion:
    - **–** Piecewise linear: hat functions
    - **–** Piecewise quadratic or cubic basis functions
    - **–** Piecewise higher order Gauss-Legendre polynomials
- Spectral and Pseudo Spectral Methods – using orthogonal global series as the basis function:
    - **–** Fourier series
    - **–** Bessel, Chebyshev, Legendre series

We'll talk about cell balance and finite element methods; in nuclear we have specific versions of these. For example, Denovo, the 3-D Cartesian mesh deterministic code from ORNL, offers these choices:

- Simplified P_N: finite volume
- Discrete ordinates: weighted diamond difference (WDD) without flux fixup is equivalent to a Crank-Nicolson method; cell balance.
- Discrete ordinates: weighted diamond difference with flux fixup to zero (WDD-FF) is a nonlinear method; cell balance
- Discrete ordinates: theta weighted diamond difference (TWD) is a nonlinear method; cell balance
- Discrete ordinates: linear discontinuous (LD) is a Galerkin method formed from the basis set $\{1, x, y, z\}$; FEM
- Discrete ordinates: bilinear discontinuous (BLD) in 2-D; FEM
- Discrete ordinates: trilinear discontinuous (TLD) is a Galerkin method formed from the basis set $\{1, x, y, z, xy, yz, xz, xyz\}$ and maintains the asymptotic diffusion limit on the grid used in Denovo; FEM
- Discrete ordinates: step characteristics (SC) in 2- or 3-D does not produce negative fluxes and does not have oscillatory behavior; can be written as a cell balance or finite element scheme

The WDD, WDD-FF, TWD, LD, BLD, and TLD schemes are all second-order, and the SC scheme is first-order.

———————————-

Aside

Galerkin Methods: Converts a continuous problem to a discrete problem - equivalent to converting the equation to a weak formulation. Typically one gives some constraints on the function space to characterize the space with a finite set of basis functions.

To get the *weak form*: rewrite a differential equation such that the equation does not contain any derivatives of the solution. You can then find solutions that are actually not differentiable. Derivatives in the original equation may not all exist, but nevertheless satisfy the equation in some specifically defined way.

————————————

LANL's PARTISN has similar choices, but their new Capsaesin code has tetrahedral mesh and uses XXXX. INL's RattleSNake uses finite element methods for YYYY.

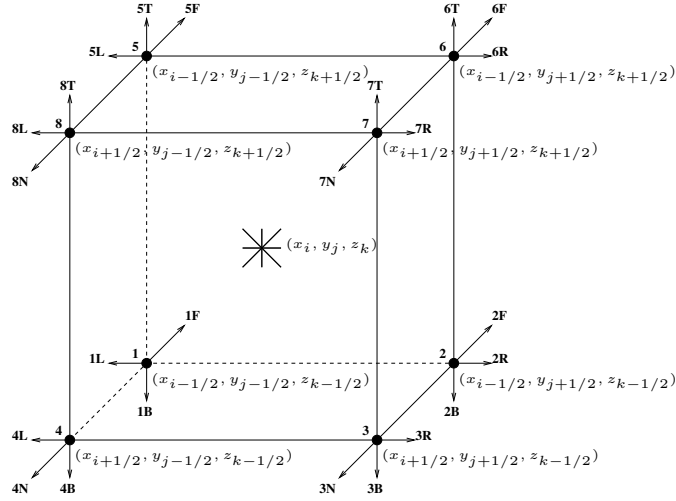We'll use the diagram in Figure 1 to think through our discretization schemes.

Figure 1: General mesh cell used to derive discrete spatial equations. The adjacent cell points are given using the notation $N \rightarrow +x$, $F \rightarrow -x$, $L \rightarrow -y$, $R \rightarrow +y$, $B \rightarrow -z$, and $T \rightarrow +z$.

For any given group, angle, and source, the transport equation can be reduced to

$$\hat{\Omega} \cdot \nabla \psi(\mathbf{r}) + \Sigma_t(\mathbf{r})\psi(\mathbf{r}) = s(\mathbf{r}) \,, \tag{1}$$

where $s(\mathbf{r})$ is a total accumulated source. In operator form, this equation is

$$\mathbf{L}\psi = s \,, \tag{2}$$

where $\mathbf{L}$ is the differential transport operator $(\hat{\Omega} \cdot \nabla + \Sigma_t(\mathbf{r}))$. We will be required to perform operations of the type

$$\psi = \mathbf{L}^{-1}s \,, \tag{3}$$

to solve discrete forms of Eq. (2).

DEFINE OPERATOR

For all the spatial differencing schemes discussed below, $\mathbf{L}$ can be *implicitly* formed as a lower-left triangular matrix and inverted by "sweeping" through the mesh in the direction of particle flow. In effect, the discretized form of Eq. (1) is solved in each cell. The outgoing fluxes become input to the downwind cells, or in other words, each cell looks "upwind" to find its incoming fluxes. Once all the incoming fluxes are defined on the entering faces of a cell, the outgoing fluxes can be calculated, and the process is repeated until the entire mesh is solved for a given angle. For each cell, the entering and exiting faces are defined by

$$\hat{\Omega} \cdot \mathbf{n} < 0 , \quad \text{(entering face)} \tag{4}$$

$$\hat{\Omega} \cdot \mathbf{n} > 0 , \quad \text{(exiting face)} . \tag{5}$$

Mathematically, this is called a *wavefront* solver. The operation $\mathbf{L}^{-1}$ is regularly referred to as a *sweep* in the nuclear engineering and transport communities.

Finite Difference

Finite Difference gives pointwise values on a grid.

We (quickly) covered the principles of finite difference when we did time discretization. We used points to approximate derivatives and were able to obtain a corresponding expression for the *Local Truncation Error* (LTE).

A note about *convergence*: the solution of the finite difference equations should converge to the true solution of the PDE as grid spacing (mesh size) goes to zero.

We're actually going to skip this formulation; I suspect you can figure it out.

Finite Volume

Finite Volume methods approximate the average integral on a reference volume. This handles discontinuities much better–why might that be? If cell boundaries line up with material boundaries and we integrate half way into each cell, we capture the impact of the neighboring materials. Thus, the cell-balance equation can be derived by integrating Eq. (1) over the mesh cell in Fig. 1, which yields a statement of conservation of particles within the mesh cell.

Weighted Diamond Difference

We will use *central difference* to approximate our spatial derivative, where 2nd order central diff is:

$$f'(x_0) = \frac{f(x_0 + h) - f(x_0 - h)}{2h} - \frac{1}{6}h^2 f'''(c_i) \,.$$

If we switch that to our system and note $x_{i+1/2} - x_i \equiv h/2$ and $x_{i+1/2} - x_{i-1/2} \equiv \Delta_i$ then we can see

$$\frac{\partial \psi}{\partial x} = \frac{\psi_{i+1/2} - \psi_{i-1/2}}{\Delta_i} - \frac{1}{6}\left(\frac{\Delta_i}{2}\right)^2 f'''(c_i) \,,$$

$$\int_{x_{i-1/2}}^{x_{i+1/2}} dx \, \frac{\partial \psi}{\partial x} \approx \frac{\psi_{i+1/2} - \psi_{i-1/2}}{\Delta_i} \,.$$

To integrate the differential term, we will note

$$\int_{x_{i-1/2}}^{x_{i+1/2}} dx \, \frac{\partial \psi}{\partial x} = \int_{x_{i-1/2}}^{x_{i+1/2}} \partial \psi = \psi_{i+1/2} - \psi_{i-1/2} \,.$$

For the other terms we will use the *midpoint integration rule*. We won't derive that rule here, but know that the midpoint rule comes from open Newton Cotes with Lagrange polynomials (a way to make integration rules) using $n = 0$ (which uses one point only):

$$\int_a^b f(x)dx = \int_{x_{i-1/2}}^{x_{i+1/2}} f(x)dx = hf(x_i) + \frac{h^3}{3}f''(\xi_i) \,.$$

For us, $x_{i+1/2} - x_{i-1/2} = h \equiv \Delta_i$. Thus, applying $\iiint (\cdot) \, dxdydz$, dividing by differential volume, and separating flux into x, y, and z components gives,

$$\frac{\mu}{\Delta_i}(\psi_{i+1/2} - \psi_{i-1/2}) + \frac{\eta}{\Delta_j}(\psi_{j+1/2} - \psi_{j-1/2}) + \frac{\xi}{\Delta_k}(\psi_{k+1/2} - \psi_{k-1/2}) + \Sigma_{t,ijk}\psi_{ijk} = s_{ijk} \,. \quad (6)$$

The derivation of the WDD equations is described in detail in Lewis & Miller. The diamond-difference method is derived by closing Eq. (6) with the average of the face-edge fluxes, which is equivalent to a Crank-Nicolson method in space. Solving the cell-balance equation with this

closure yields the following system of equations,

$$\mu \gtrless 0 \,, \eta \gtrless 0 \,, \xi \gtrless 0$$

$$\psi_{ijk} = \frac{s_{ijk} + \frac{2}{(1\pm\alpha_i)}\frac{|\mu|}{\Delta_i}\bar{\psi}_{i\mp1/2} + \frac{2}{(1\pm\alpha_j)}\frac{|\eta|}{\Delta_j}\bar{\psi}_{j\mp1/2} + \frac{2}{(1\pm\alpha_k)}\frac{|\xi|}{\Delta_k}\bar{\psi}_{k\mp1/2}}{\Sigma_{ijk} + \frac{2}{(1\pm\alpha_i)}\frac{|\mu|}{\Delta_i} + \frac{2}{(1\pm\alpha_j)}\frac{|\eta|}{\Delta_j} + \frac{2}{(1\pm\alpha_k)}\frac{|\xi|}{\Delta_k}} \,,$$

$$\psi_{i\pm1/2} = \frac{2}{(1\pm\alpha_i)}\psi_{ijk} - \frac{(1\mp\alpha_i)}{(1\pm\alpha_i)}\bar{\psi}_{i\mp1/2} \,, \tag{7}$$

$$\psi_{j\pm1/2} = \frac{2}{(1\pm\alpha_j)}\psi_{ijk} - \frac{(1\mp\alpha_j)}{(1\pm\alpha_j)}\bar{\psi}_{j\mp1/2} \,,$$

$$\psi_{k\pm1/2} = \frac{2}{(1\pm\alpha_k)}\psi_{ijk} - \frac{(1\mp\alpha_k)}{(1\pm\alpha_k)}\bar{\psi}_{k\mp1/2} \,.$$

Here, the $\bar{\psi}$ are the incoming fluxes on each face. The α terms are weighting factors such that $\alpha = 0$ gives the classic diamond-difference equations and $\alpha = \pm1$ gives the step-difference equations. Setting $\alpha = \pm1$ yields a first-order spatial differencing scheme. The default behavior of Denovo for WDD uses $\alpha = 0$, which gives the diamond-difference method.

Many codes, like Denovo, provide a version of WDD that can correct negative fluxes. When the outgoing flux is less than zero, we set the face-edge flux to zero and recalculate ψ_{ijk} and the new edge fluxes. This process is repeated until all the outgoing fluxes are greater than or equal to zero. This method is nonlinear in that the corrected solution of Eq. (7) depends on ψ.

Theta Weighted Diamond

Another nonlinear cell-balance scheme is TWD. This scheme uses the incoming fluxes to calculate weighting factors that permit the calculation of cell-centered and outgoing fluxes that vary smoothly between the step and diamond-difference approximations. The weighting factors are calculated from the following system of equations,

$$\mu \gtrless 0 \,, \eta \gtrless 0 \,, \xi \gtrless 0$$

$$1 - a = \frac{s_{ijk}V\theta_s + (|\eta|B\bar{\psi}_{j\mp1/2} + |\xi|C\bar{\psi}_{k\mp1/2})\theta + |\mu|A\bar{\psi}_{i\mp1/2}}{(\Sigma_{ijk}V + 2|\eta|B + 2|\xi|C)\bar{\psi}_{i\mp1/2}} \,,$$

$$1 - b = \frac{s_{ijk}V\theta_s + (|\mu|A\bar{\psi}_{i\mp1/2} + |\xi|C\bar{\psi}_{k\mp1/2})\theta + |\eta|B\bar{\psi}_{j\mp1/2}}{(\Sigma_{ijk}V + 2|\mu|A + 2|\xi|C)\bar{\psi}_{j\mp1/2}} \,, \tag{8}$$

$$1 - c = \frac{s_{ijk}V\theta_s + (|\mu|A\bar{\psi}_{i\mp1/2} + |\eta|B\bar{\psi}_{j\mp1/2})\theta + |\xi|C\bar{\psi}_{k\mp1/2}}{(\sigma_{ijk}V + 2|\mu|A + 2|\eta|B)\bar{\psi}_{k\mp1/2}} \,,$$

where

$$A = \Delta_j \Delta_k , \quad B = \Delta_i \Delta_k , \quad C = \Delta_i \Delta_j , \quad V = \Delta_i \Delta_j \Delta_k . \tag{9}$$

The theta-weighting factors, θ and θ_s, are set to values between 0 and 1. By default Denovo uses the *theta-weighted* model from the TORT code in which $\theta = \theta_s = 0.9$.

The weighting parameters are bounded between the diamond-difference and step approximations,

$$\frac{1}{2} \leq \{a, b, c\} \leq 1 . \tag{10}$$

Using these factors, the cell-centered and outgoing fluxes are

$$
\begin{aligned}
\psi_{ijk} &= \frac{s_{ijk}V + \frac{|\mu|A}{a}\bar{\psi}_{i\mp 1/2} + \frac{|\eta|B}{b}\bar{\psi}_{j\mp 1/2} + \frac{|\xi|C}{c}\bar{\psi}_{k\mp 1/2}}{s_{ijk}V + \frac{|\mu|A}{a} + \frac{|\eta|B}{b} + \frac{|\xi|C}{c}} , \\
\psi_{i\pm 1/2} &= \frac{1}{a}\psi_{ijk} - \frac{(1-a)}{a}\bar{\psi}_{i\mp 1/2} , \\
\psi_{j\pm 1/2} &= \frac{1}{b}\psi_{ijk} - \frac{(1-b)}{b}\bar{\psi}_{j\mp 1/2} , \\
\psi_{k\pm 1/2} &= \frac{1}{c}\psi_{ijk} - \frac{(1-c)}{c}\bar{\psi}_{k\mp 1/2} .
\end{aligned}
\tag{11}
$$

TWD and WDD-FF produce uniformly positive fluxes when the source, s_{ijk}, is greater than zero.

Finite Element

Finite element schemes are derived from the weak form of Eq. (1). We begin the derivation by integrating Eq. (1) over a single element, e, and multiplying by a weighting function for the element, w_{en},

$$\int_{V_e} w_{en}(\hat{\Omega} \cdot \nabla\psi + \sigma\psi) \, dV = \int_{V_e} w_{en}s \, dV , \tag{12}$$

where the element defined in Fig. 1 has $dV = dxdydz$. The weight functions are defined over the range $n \in [1, N]$ such that the set w_{en} is linearly independent. Furthermore, we make the assumption that all elements in the orthogonal grid have equal weight functions, so $w_{en} \equiv w_n$. Applying Green's theorem to the gradient term gives the weak form of the transport equation,

$$\oint_{\partial V_e} w_n \hat{\mathbf{n}} \cdot \hat{\Omega}\psi \, dA - \int_{V_e} \hat{\Omega} \cdot \nabla w_n \psi \, dV + \int_{V_e} w_n \Sigma_t \psi \, dV_e = \int_{V_e} w_n s \, dV , \quad n = 1, \dots, N . \tag{13}$$

Now, we expand the angular flux in the following basis,

$$\psi = \sum_{m=1}^{N} b_m(\mathbf{r}) \psi_e^{(m)} \,, \quad \mathbf{r} \in \partial V_e \,. \tag{14}$$

Applying the Galerkin finite element approximation in which $w_n = b_n$, Eq. (13) becomes

$$\oint_{\partial V_e} b_n \hat{\mathbf{n}} \cdot \hat{\Omega} \psi \, dA - \mathcal{T}\Psi + \Sigma_e \mathcal{M}\Psi = \mathcal{M}S \,, \tag{15}$$

where the elements of the matrices and vectors are defined

$$[\mathcal{T}]_{nm} = \int_{V_e} \hat{\Omega} \cdot \nabla b_n b_m \, dV \,,$$

$$[\mathcal{M}]_{nm} = \int_{V_e} b_n b_m \, dV \,,$$

$$\Psi = \begin{pmatrix} \psi_e^{(1)} & \psi_e^{(2)} & \cdots & \psi_e^{(N)} \end{pmatrix}^T \,, \tag{16}$$

$$S = \begin{pmatrix} s_e^{(1)} & s_e^{(2)} & \cdots & s_e^{(N)} \end{pmatrix}^T \,,$$

and the source has been expanded in the same basis as the angular flux. The angular fluxes in the surface term come from upwind cells or boundary conditions.

The size and composition of the matrices in Eq. (15) are dependent on the mesh and the basis functions chosen to represent the unknowns.

Linear Discontinuous

The LD method defines a basis over the set $\{1, x, y, z\}$ with the shape functions [**?**],

$$b_1 = 1 \,, \quad b_2 = \frac{2(x - x_{ijk})}{\Delta_i} \,, \quad b_3 = \frac{2(y - y_{ijk})}{\Delta_j} \,, \quad b_4 = \frac{2(z - z_{ijk})}{\Delta_k} \,. \tag{17}$$

Using these shape functions in Eq. (15) and analytically evaluating the integrals give the following system of equations,

$$
\frac{\mu}{\Delta_i}(\psi_{i+1/2} - \psi_{i-1/2}) + \frac{\eta}{\Delta_j}(\psi_{j+1/2} - \psi_{j-1/2}) + \frac{\xi}{\Delta_k}(\psi_{k+1/2} - \psi_{k-1/2}) + \Sigma_t \psi^a = s^a ,
$$

$$
\frac{3\mu}{\Delta_i}(\psi_{i+1/2} + \psi_{i-1/2} - 2\psi^a) + \frac{\eta}{\Delta_j}(\psi^x_{j+1/2} - \psi^x_{j-1/2}) + \frac{\xi}{\Delta_k}(\psi^x_{k+1/2} - \psi^x_{k-1/2}) + \Sigma_t \psi^x = s^x ,
$$

$$
\frac{\mu}{\Delta_i}(\psi^y_{i+1/2} - \psi^y_{i-1/2}) + \frac{3\eta}{\Delta_j}(\psi_{j+1/2} + \psi_{j-1/2} - 2\psi^a) + \frac{\xi}{\Delta_k}(\psi^y_{k+1/2} - \psi^y_{k-1/2}) + \Sigma_t \psi^y = s^y ,
$$

$$
\frac{\mu}{\Delta_i}(\psi^z_{i+1/2} - \psi^z_{i-1/2}) + \frac{\eta}{\Delta_j}(\psi^z_{j+1/2} - \psi^z_{j-1/2}) + \frac{3\xi}{\Delta_k}(\psi_{k+1/2} + \psi_{k-1/2} - 2\psi^a) + \Sigma_t \psi^z = s^z .
$$

(18)

Here,

$$
\psi^{(1)}_e = \psi^a , \quad \psi^{(2)}_e = \psi^x , \quad \psi^{(3)}_e = \psi^y , \quad \psi^{(4)}_e = \psi^z ,
$$

(19)

such that ψ^a is the average angular flux in the element and $\psi^{x|y|z}$ are the slopes in the (x, y, z) directions. The same notation is used for the expanded source, s.

Equations (14) and (17) are used to develop upwind expressions for ψ,

$$
\psi_{i\pm1/2} = \psi^a \pm \psi^x , \quad \psi_{j\pm1/2} = \psi^a \pm \psi^y , \quad \psi_{k\pm1/2} = \psi^a \pm \psi^z , \quad \{\mu, \eta, \xi\} \gtrless 0 ,
$$

(20)

and the upwinded slopes are

$$
\psi^{(y|z)}_{i\pm1/2} = \psi^{(y|z)} , \quad \psi^{(x|z)}_{j\pm1/2} = \psi^{(x|z)} , \quad \psi^{(x|y)}_{k\pm1/2} = \psi^{(x|y)} .
$$

(21)

For each direction, these expressions are inserted into Eq. (18), and the resulting 4×4 system is solved for Ψ. For efficiency, the solution to the matrix is precomputed, and Ψ is calculated by evaluating four statements.

TriLinear Discontinuous

The TLD method is the only spatial discretization that maintains the asymptotic diffusion limit on the grid used. The TLD equations are derived by expanding Ψ in the basis

$$
\{1, x, y, z, xy, yz, xz, xyz\} .
$$

9

thus, there are eight unknowns per cell. We define the unknowns at each node of the cell as indicated by the cardinal numbers in Fig. 1. The basis functions are

$$b_1 = \left(\frac{x_{i+1/2} - x}{\Delta_i}\right)\left(\frac{y_{j+1/2} - y}{\Delta_j}\right)\left(\frac{z_{k+1/2} - z}{\Delta_k}\right),$$
$$b_2 = \left(\frac{x_{i+1/2} - x}{\Delta_i}\right)\left(\frac{y - y_{j-1/2}}{\Delta_j}\right)\left(\frac{z_{k+1/2} - z}{\Delta_k}\right),$$
$$b_3 = \left(\frac{x - x_{i-1/2}}{\Delta_i}\right)\left(\frac{y - y_{j-1/2}}{\Delta_j}\right)\left(\frac{z_{k+1/2} - z}{\Delta_k}\right),$$
$$b_4 = \left(\frac{x - x_{i-1/2}}{\Delta_i}\right)\left(\frac{y_{j+1/2} - y}{\Delta_j}\right)\left(\frac{z_{k+1/2} - z}{\Delta_k}\right),$$
$$b_5 = \left(\frac{x_{i+1/2} - x}{\Delta_i}\right)\left(\frac{y_{j+1/2} - y}{\Delta_j}\right)\left(\frac{z - z_{k-1/2}}{\Delta_k}\right), \tag{22}$$
$$b_6 = \left(\frac{x_{i+1/2} - x}{\Delta_i}\right)\left(\frac{y - y_{j-1/2}}{\Delta_j}\right)\left(\frac{z - z_{k-1/2}}{\Delta_k}\right),$$
$$b_7 = \left(\frac{x - x_{i-1/2}}{\Delta_i}\right)\left(\frac{y - y_{j-1/2}}{\Delta_j}\right)\left(\frac{z - z_{k-1/2}}{\Delta_k}\right),$$
$$b_8 = \left(\frac{x - x_{i-1/2}}{\Delta_i}\right)\left(\frac{y_{j+1/2} - y}{\Delta_j}\right)\left(\frac{z - z_{k-1/2}}{\Delta_k}\right).$$

Substituting these into Eq. (15) and evaluating the integrals analytically, we derive the TLD equations for the cells. We are skipping this because it's a mess and waaay more than we need.

1   Step Characteristics

The primary advantage of the SC scheme is that it produces uniformly positive solutions. SC gives positive fluxes as long as the source is positive, and it does not require non-linear flux fix-ups like WDD-FF or TWD. Also, it does not suffer from oscillatory behavior like step differencing. Because of these properties, SC is an ideal choice for calculating adjoint importance maps for use in hybrid Monte Carlo methods. However, if very high accuracy is required, LD and TLD are better choices because they are second-order methods, whereas SC is first-order.

The SC spatial discretization can be derived using the cell-balance or finite element formalism. We will use the slice-balance method originally proposed by Lathrop [**?**]. First, define a minimum step size through the cell defined in Fig. 1,

$$d = \min\left(\frac{\Delta_i}{|\mu|}, \frac{\Delta_j}{|\eta|}, \frac{\Delta_k}{|\xi|}\right). \tag{23}$$

We now define a new set of indices, $\{i, j, k\} \rightarrow \{p, q, r\}$, such that p is associated with the index of d, and $\{q, r\}$ are associated with the remaining indices. The slice fluxes are defined

$$
\begin{aligned}
\psi_0^m &= \bar{s} + e^{-\Sigma_t d}(\psi_{\text{inc}}^m - \bar{s}) \,, \\
\psi_1^m &= \bar{s} + \frac{1}{\Sigma_t d}(\psi_{\text{inc}}^m - \psi_0^m) \,, \\
\psi_2^m &= \bar{s} + \frac{2}{\Sigma_t d}(\psi_{\text{inc}}^m - \psi_1^m) \,, \\
m &= p, q, r \,,
\end{aligned}
\tag{24}
$$

and $\bar{s} = s/\Sigma_t$. For each slice a normalized distance is defined,

$$
\delta_m = \left(\frac{|\hat{\Omega}|_m}{\Delta_m} \right) d \,,
\tag{25}
$$

such that $\delta_p = 1$ and $\delta_{q,r} \leq 1$. The areas of each slice are

$$
A_{pq} = \frac{\delta_p \delta_r}{2} \,, \quad B_{pq} = \delta_p(1 - \delta_r) \,, \quad C_{pp} = (1 - \delta_q)(1 - \delta_r) \,.
\tag{26}
$$

By using these definitions, the outgoing fluxes are

$$
\begin{aligned}
\psi_p &= A_{qp}\psi_2^q + A_{rp}\psi_2^r + B_{qp}\psi_1^q + B_{rp}\psi_1^r + C_{pp}\psi_0^p \,, \\
\psi_q &= A_{pq}\psi_2^p + A_{rq}\psi_2^r + B_{pq}\psi_1^p \,, \\
\psi_r &= A_{pr}\psi_2^p + A_{qr}\psi_2^q + B_{pr}\psi_1^p \,.
\end{aligned}
\tag{27}
$$

Finally, the cell-centered flux is

$$
\psi = \bar{s} + \frac{1}{\Sigma_t d} \sum_m \delta_m(\psi_{\text{inc}}^m - \psi_m) \,, \quad m = p, q, r \,.
\tag{28}
$$

Because these equations depend inversely on $\Sigma_t d$, we need to handle cases where $\Sigma_t d \ll 1$, which includes vacuum regions. In Denovo, when $\Sigma_t d \leq 0.025$ we expand $\exp(-\Sigma_t d)$ in a $O(7)$ Taylor-series. Using the expansion in Eqs. (24) through (28) yields formulas for the outgoing and cell-centered flux that do not vary inversely proportional to $\Sigma_t d$.